Aircraft Damage Identification and Classification for Database-driven Online Safe Flight Envelope Prediction

Zhang, Y; de Visser, CC; Chu, QP

Important note
To cite this publication, please use the final published version (if applicable).
Please check the document version above.

Aircraft Damage Identification and Classification for Database-Driven Online Flight-Envelope Prediction

Y. Zhang,* C. C. de Visser,† and Q. P. Chu‡

Delft University of Technology, 2629 HS Delft, The Netherlands

Safe flight-envelope prediction is essential for preventing aircraft loss of control after the occurrence of sudden structural damage and aerodynamic failures. Considering the unpredictable nature of such failures, many challenges remain in the process of implementing such a prediction system. In this paper, an approach to online safe flight-envelope prediction is proposed that is based on the retrieval of information from offline-assembled databases. One of the key steps of this approach is determining the structural damage of the state of the aircraft by using the identification, detection, and classification methods presented in this paper. The estimated damage cases will lead to structural damage indices in the database corresponding to those safe flight envelopes that are "closest" to the actual safe flight envelope of the damaged aircraft. The feasibility of the proposed database-driven approach is proved by simulation results, where three damage cases are successfully detected and classified.

Nomenclature

A_x, A_y, A_z	=	specific forces along the body X, Y, or Z axes, m/s^2
b	=	wingspan, m
C	=	dimensionless aerodynamic coefficient
$\bar{c}$	=	mean aerodynamic chord, m
$I_{xx}, I_{yy}, I_{zz}, I_{xz}$	=	moments and products of inertia
L, M, N	=	aerodynamic moments along the body X, Y, or Z axes, N · m
p, q, r	=	roll, pitch, and yaw rate around the body X, Y, or Z axes, rad/s
S	=	wing area, s^2
V	=	airspeed, m/s
X, Y, Z	=	aerodynamic forces along the body X, Y, or Z axes, N
$\boldsymbol{x}$	=	training example vector
$\boldsymbol{y}$	=	training target vector
α	=	angle of attack, rad
β	=	angle of sideslip, rad
$\delta_a, \delta_e, \delta_r$	=	control surface deflections of aileron, elevator, and rudder, rad
ρ	=	air density, kg/m^3

I. Introduction

AIRCRAFT loss of control (LOC) has remained one of the dominant causes of fatal aircraft accidents over the past few decades [1,2]. LOC accidents are generally related to a significant deviation of the aircraft from the nominal flight envelope due to external hazards, technical failures, and pilot error [3].

The safe flight envelope (SFE) is characterized by aerodynamic and kinematic models of the aircraft as well as control authority, and it represents the region in the state space in which the aircraft can be safely operated. Different definitions of the flight envelope are proposed in the literature; see, e.g., [4–9]. Widely used to prevent stall and potential structural damage, the conventional maneuvering envelope defines hard constraints on the speed and load factor.

In addition to these static limitations, dynamic envelope bounds can be established by determining the controllable or reachable states, given the control authority of the pilot or autopilot [5,6]. A reachability analysis provides a rigorous approach to actually calculate the dynamic envelope bounds [5,6]. In principle, a reachability analysis determines the complete set of states that can be reached from a target set within a given time horizon while subject to the system dynamics and input constraints. If the dynamics of the system are nonlinear, as is the case with aircraft, a nonlinear reachability analysis approach must be used [6]. A nonlinear reachability analysis defines the SFE as the intersection between a forward reachable set and a backward reachable set; see Fig. 1. This intersection indicates the region in the state space, inside which the aircraft is guaranteed to be capable of maneuvering from as well as returning to a trim set within a certain time horizon [7–9].

During nominal flight, these envelopes can be stored as a fixed part of a LOC prevention system [4]. However, they may no longer be valid after sudden failures or structural damage because the aerodynamic properties of the damaged aircraft would change: often significantly. For example, under the situation of wing damage, the maximum lift coefficient decreases, which results in a higher stall speed and lower maximum load factor. Therefore, the overall maneuvering envelope will shrink due to the change in the aerodynamic coefficients, as is illustrated in Fig. 1. Under such abnormal conditions, the pilots need to acquire the reduced SFE as quickly as possible, implying that the onboard computer must recalculate the solution in near-real time.

Two significant challenges exist when updating the SFE based on reachable sets. The first, called the fundamental challenge, is the result of the fact that a nonlinear reachability analysis requires an accurate global model of the aircraft dynamics to compute an accurate SFE. In the presence of failures and damage, measurement data required for online system identification can realistically only be obtained in a limited region around the current flight condition because the impaired aircraft may not be able to maneuver freely without exiting the new SFE, thereby causing the very problem the system is intended to prevent. Hence, the onboard global model can only be updated locally in the direct neighborhood of the current flight state, with the remainder of the global model necessarily assumed unchanged. Without a valid global model, however, the computed SFE using nonlinear reachability analysis will be inaccurate.
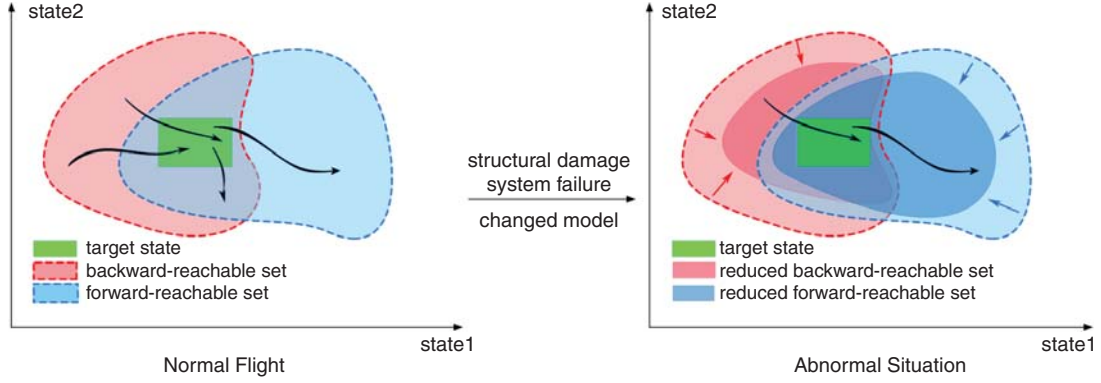
The second challenge is more practical in nature, and it is the result of the very high computational cost of computing the SFE using a nonlinear reachability analysis with a realistic aircraft model. All current approaches suffer from the so-called curse of dimensionality,

4 **Fig. 1   Safe flight envelope and its change after sudden damage and failures.**

in the sense that they scale badly (i.e., exponentially) with increasing state-space dimension, rendering them infeasible for online implementations.

The solution that is proposed in this paper is to consider retrieving the SFE from an onboard database that is constructed offline and contains the precomputed SFEs for various representative fault and damage scenarios. For each representative damage case, a global dynamics model and its corresponding SFE are computed offline and then stored in the database. Only database retrieval is performed online, thereby circumventing the two aforementioned challenges associated with direct online SFE prediction. One of the key steps of this approach is to determine the index into the database, given an indication of potential abnormal conditions of sensors, actuators, and airframe.

In aerospace engineering, fault detection and isolation (FDI) methods are intensively used in monitoring and diagnosing the health **5** of aircraft sensors and actuators, as well as providing updated information for control systems [11]. In general, FDI methods rely on either hardware redundancy or analytical redundancy [12]. Sensor faults are usually diagnosed by a hardware redundancy approach, whereas faults in actuators are detected based on mathematical models and estimation techniques. These techniques have been well developed and applied to aircraft [13]; in this paper, it is therefore assumed that faults in sensors and actuators are detected by advanced FDI systems. The problem this paper seeks to address is the assessment of the structural integrity of aircraft after sudden damage, like the partial loss of wings and tails. This issue has not received much attention in the literature.

One reason for this is that repeated destructive experiments on large-scale structures like aircraft are very costly at best and infeasible **6** at worst; as a result, there are very limited data available for analysis. However, a number of nondestructive computational fluid dynamics (CFD) and wind-tunnel experiments have been conducted [14–17] to satisfy the expanding need for damaged aircraft models. Moreover,

there is ample literature on nondestructive structural health monitoring (SHM) techniques [11,18,19] using vibration-based inputs, mode shape curvatures, and material properties based on finite element models.

Inspired by the techniques and methods used in SHM, a different approach for online detection and classification of structural damage is proposed in this paper based on a framework for machine learning and pattern classification [20]. The featured inputs to the classifier are the stability derivatives identified from the well-known "two-step method" [21]. In this way, structural damage to any main part of the aircraft can be detected and estimated. Accordingly, the estimation result is used to generate an index into the database with stored SFEs. The retrieved envelope will then be used to drive an adaptive envelope protection system.

The contribution of this paper is a novel procedure for online classification of structural damage from locally estimated aerodynamic parameters after failure occurrence. The results from the classification are used to access a database containing stored SFEs for different representative damage cases. The novel procedure is **7** thus a key element of the database-driven online safe flight-envelope prediction method, indicated as "DEFEND."

The paper has the following outline. In Sec. II, a general framework of the DEFEND system is given. In Sec. III, the process of aerodynamic parameter identification based on a two-step method is introduced. The methods of aerodynamic anomaly detection and damage classification using identification results are proposed in Sec. IV. The method is demonstrated and validated through simulation results shown in Sec. V. Finally, in Sec. VI, the future work of a database retrieval method is briefly introduced, followed by discussions and conclusions in Secs. VII and VIII.

II.   System Overview

The general process of the DEFEND system is illustrated in Fig. 2, where the onboard system is supported by two offline databases. It is
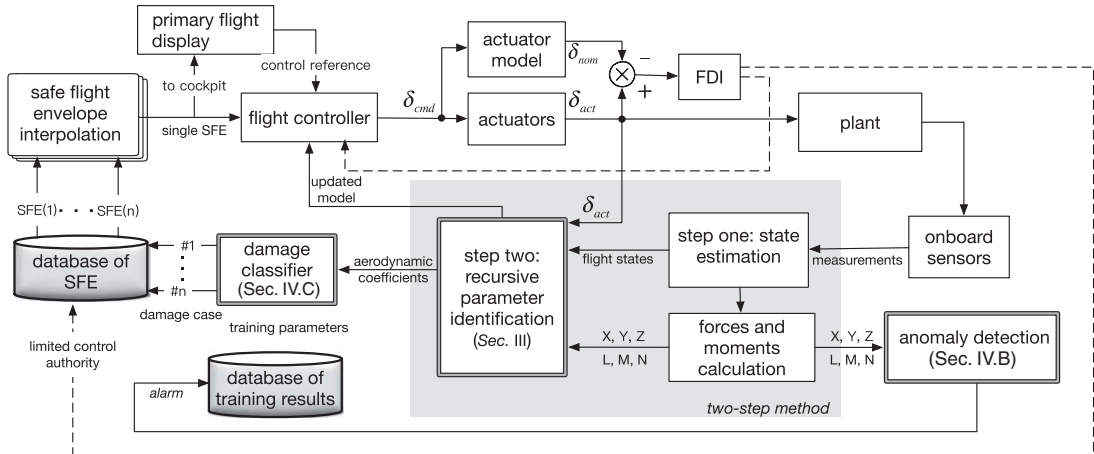
Fig. 2   General framework of DEFEND: a database-driven safe flight-envelope prediction system.

clearly shown that the realization of online SFE prediction is strongly connected to the database retrieval system, and a reliable online identification process is essential for successful retrieval from the database. As displayed in Fig. 2, commands from the onboard flight controller are first sent to flight actuators as well as the FDI module to monitor the health conditions of the actuators. If any failure happens (e.g., hardover, jam), it will soon be detected by abnormal residuals between the actual outputs of actuators and the expected values calculated from their mathematical models [12]. Meanwhile, onboard sensors are also being monitored by advanced FDI techniques, such that any sensor faults can be quickly detected and compensated for [13]. New measurements of flight states and responses are sent to the system identification module, which uses the two-step method [21] to update the aircraft model. At the first step, the aircraft states and the sensor bias are estimated by a Kalman filter or other advanced state estimators based on aircraft kinematic models.

Next, the nondimensional forces and moments along each axis are calculated using the estimated states and sensor information, which provides the input to the second step of the two-step method, i.e., the estimation of stability derivatives by using a recursive least-squares method. For damaged aircraft, it is likely that the conventional model structure has changed, so a model structure selection scheme is used [22]. According to a series of experiments and reports [14–17], the aerodynamic model is directly related to the integrity of the airplane's components and structures. Hence, the calculated dimensionless forces and moments are used to initiate an online aerodynamic anomaly detection process, which works by comparing the output of nominal flight models with the current output measurements. If there are any abnormal changes to the forces and moments, control inputs will be given in an effort to counteract the induced motion, creating the sufficient input excitation needed for the identification of the changed local model. Meanwhile, an alarm will be generated that triggers the damage classification to determine the position and scale of the possible damage based on the newly identified stability derivatives. However, online identification can only update the model in a local region around the current state due to the limited excitation provided by small maneuvers after damage. The onboard classification process needs to retrieve the offline training knowledge of various global damage models and flight conditions stored in the database. Once the damage case is estimated, this information will be provided to the database as an index to retrieve a set of candidate SFEs. By applying database retrieval schemes and interpolation algorithms, a unique SFE is obtained that is closest to the current damage situation. The obtained SFE can then be presented to the pilots and used by the fault-tolerant controller to generate new control laws.

Under this general framework, the focus of this paper is the damage detection and classification based on estimated nondimensional aerodynamic coefficients (double-framed blocks in Fig. 2), which will be thoroughly discussed in Secs. IV and V with simulation results. Additionally, future work on database retrieval and SFE interpolation methods (shaded blocks in Fig. 2) is introduced in Sec. VI, which will complete the loop of the DEFEND system.

III. Aerodynamic Parameter Identification

The precondition of a reliable online envelope prediction system is an accurate plant model, which is obtained by an efficient system identification method. The method used in this paper is the two-step method in the time domain, where the estimation of flight states and aerodynamic coefficients are separately dealt with. Because the research is aimed at classifying aircraft structural damage, the focus is on the second step of the two-step method, in which the identification of changed aerodynamic coefficients is key to diagnosing damage.

The aircraft model used in this paper, shown as the plant in Fig. 2, is the Cessna Citation laboratory aircraft (abbreviated as PH-LAB) operated by the Delft University of Technology and The Netherlands's National Aerospace Laboratory/NLR. The PH-LAB is a twin-jet business aircraft designed and constructed by the aircraft manufacturer Cessna [23]. In this paper, the aerodynamic model of the PH-LAB is identified from the online input/output flight data generated by a high-fidelity MATLAB/SIMULINK environment, which incorporates the nonlinear aircraft model with aerodynamic lookup tables identified from real flight tests (Fig. 3) [24]. The simulation environment is called "DASMAT," which is the acronym for "Delft University aircraft simulation model and analysis tool." DASMAT is used in our research to simulate, analyze, and compare the dynamic behavior of damaged and undamaged aircraft, given different control inputs and strategies [25]. During the simulation, it is assumed that the generated flight states have been preprocessed by the state estimation step and that the measurements are free from sensor bias and external disturbances. The simulated states are then used to calculate the dimensionless aerodynamic forces and moments of the aircraft [22]:

$$\begin{bmatrix} C_L \\ C_D \\ C_Y \end{bmatrix} = \begin{bmatrix} \sin\alpha & 0 & -\cos\alpha \\ -\cos\alpha & 0 & -\sin\alpha \\ 0 & 1 & 0 \end{bmatrix} \begin{bmatrix} \frac{mA_x}{1/2\rho V^2 S} \\ \frac{mA_y}{1/2\rho V^2 S} \\ \frac{mA_z}{1/2\rho V^2 S} \end{bmatrix} \quad (1)$$

$$C_l = \frac{\dot{p}I_{xx} + qr(I_{zz} - I_{yy}) - (pq + \dot{r})I_{xz}}{(1/2)\rho V^2 Sb}$$

$$C_m = \frac{\dot{q}I_{yy} + rp(I_{xx} - I_{zz}) + (p^2 - r^2)I_{xz}}{(1/2)\rho V^2 S\bar{c}}$$

$$C_n = \frac{\dot{r}I_{zz} + pq(I_{yy} - I_{xx}) + (qr - \dot{p})I_{xz}}{(1/2)\rho V^2 Sb} \quad (2)$$

The effect of the structural damage is mainly a combination of aerodynamic changes and mass (and inertia) shifts [26]. However,
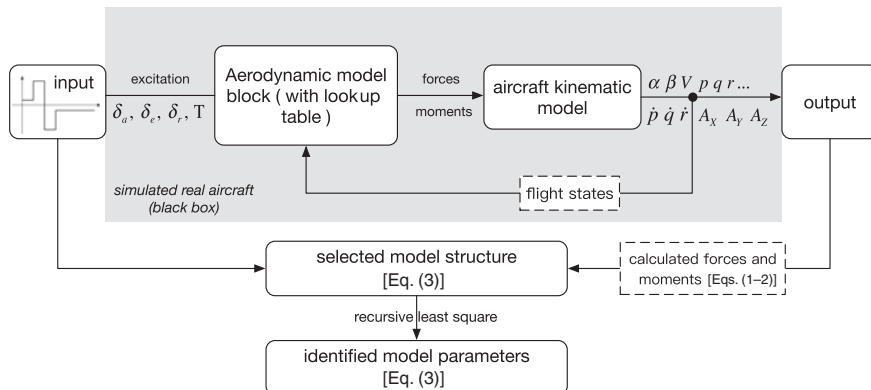

Fig. 3   System identification based on the input/output data generated from the simulation environment.

mass properties, although coupled with forces and moments, seem not to have a substantial effect on flight characteristics relative to the aerodynamic and control effects, which is according to recent wind-tunnel experiments in which a large asymmetric mass change (physical separation of an engine) was modeled [15]. Directly measuring or even numerically estimating changed mass properties after structural damage is currently not feasible. However, the damage detection and classification method presented in this paper does not necessarily require the exact value of the forces and moments, but only the aerodynamic effects of the damage. In this sense, the effects of changed the weight and inertia are lumped with that of the aerodynamic changes, and the mass and inertia in Eqs. (1) and (2) are assumed constant.

According to Fig. 3, the calculated dimensionless coefficients are used to identify the aerodynamic model parameters. Because, in real flight as well as in DASMAT simulations, the aerodynamic models are black box, a model structure needs to be estimated through a model selection scheme based on the input and output data. The model structure in Eq. (3) is selected for identifying the aerodynamic model of the Citation aircraft from simulation data, where each model parameter corresponds to one of the control and stability derivatives:

$$C_L = C_{L_0} + C_{L_\alpha}\alpha + C_{L_q}\frac{q\bar{c}}{V} + C_{L_{\delta_e}}\delta_e$$

$$C_D = C_{D_0} + C_{D_\alpha}\alpha + C_{D_{\alpha^2}}\alpha^2 + C_{D_q}\frac{q\bar{c}}{V} + C_{D_{\delta_e}}\delta_e$$

$$C_Y = C_{Y_0} + C_{Y_\beta}\beta + C_{Y_p}\frac{pb}{2V} + C_{Y_r}\frac{rb}{2V} + C_{Y_{\delta_a}}\delta_a + C_{Y_{\delta_r}}\delta_r$$

$$C_l = C_{l_0} + C_{l_\beta}\beta + C_{l_p}\frac{pb}{2V} + C_{l_r}\frac{rb}{2V} + C_{l_{\delta_a}}\delta_a + C_{l_{\delta_r}}\delta_r + C_{l_\alpha}\alpha$$

$$C_m = C_{m_0} + C_{m_\alpha}\alpha + C_{m_q}\frac{q\bar{c}}{V} + C_{m_{\delta_e}}\delta_e$$

$$C_n = C_{n_0} + C_{n_\beta}\beta + C_{n_p}\frac{pb}{2V} + C_{n_r}\frac{rb}{2V} + C_{n_{\delta_a}}\delta_a + C_{n_{\delta_r}}\delta_r \qquad (3)$$

The estimation method used in this paper is a recursive least-squares method. Variable forgetting factors are used to enhance the influence of new data when the model parameters suddenly change, as well as mitigating covariance matrix saturation under a steady-state condition. A more in-depth coverage of this technique can be found in [27].

IV. Damage Detection and Classification

To ensure the reliability and safety of the aircraft, an onboard health monitoring and assessment system is essential. Most malfunctions normally occur in engines, sensors, and actuators, as well as airframe components like wings and tails [3]. Because onboard devices and indicators have been developed in the past for various failures [12] in engines, actuators, and sensors [13], this is outside the scope of the current research. Instead, the main focus of this paper is on structural failures (i.e., the damage to a certain part of the airframe or actuators, where the aerodynamics change on a global scale), and the stability derivatives related to the structures need to be reidentified. Because the global aerodynamic model is not influenced by other nonstructural failures, the damage assessment can be performed independently.

Structural health monitoring techniques for large plants are an active field of research [19]. SHM techniques aim to detect and classify component faults like fatigue cracks, friction, and loose joints by applying machine learning algorithms [28] like neural networks and fuzzy logic on observation data acquired from large arrays of sensors. However, conventionally used vibration-based techniques employed in SHM are currently not available for aircraft due to the lack of necessary sensors. Moreover, a failure has occurred, it is more useful from the perspective of flight-envelope prediction if the structural damage is assessed on a higher level, i.e., to decide which "main" part of the aircraft (e.g., fuselage, wings, vertical tail) has been compromised.

Inspired by the techniques and methods used in SHM [11], this section proposes a novel way of detecting and classifying aircraft damage by using locally estimated aerodynamic stability derivatives to offline train a damage classifier with a supervised learning approach [20]. The data for offline training are obtained by running dynamic simulation experiments based on several predefined structural damage cases. During training, the classifier produces decision boundaries or surfaces that divide the measurement space into several damage class regions. After training, the classifier uses online estimated aerodynamic stability derivatives to assign, in real time, the current damage condition to one of the damage class regions. As a proof of concept of the new approach, three representative damage categories are chosen: horizontal stabilizer damage, vertical tail damage, and wing damage.

A. Aerodynamic Effect Modeling of Structural Damage

To determine the damage class, the aerodynamic characteristics of each damage case must be modeled as accurately as possible. In the "ideal" case, this requires data from systematically conducted flight experiments with damaged aircraft that, for obvious reasons, are problematic to obtain. Most experiments are therefore based on subscale models in the wind-tunnel [17] and CFD experiments [29]. In recent years, the generic transport model (GTM), which is a 5.5% scale model of a commercial aircraft, has been the subject of a series of extensive wind-tunnel tests undertaken by NASA [14,15] for the exploration of loss-of-control events [16]. In these experiments, the damage was modeled in the form of partial or complete tip loss of the three major parts of the subscale GTM model that provided the aerodynamic forces and moments: the horizontal stabilizers, the vertical tail, and the wings. Also, preliminary work on damage modeling has also been performed using digital DATCOM, where the aerodynamic characteristic of a Cessna Citation aircraft with various levels of vertical tail damage was modeled [30].

It can be concluded from these experiments that each damage case results in unique aerodynamic effects on the aircraft and changes in different stability derivatives. The experimental results of horizontal stabilizer damage [14] show that the damage causes significant changes to longitudinal stability, which is indicated by the changed value of C_{m_α} and C_{m_q}. Additionally, due to geometric asymmetry, a slight incremental rolling moment is observed with the increasing value of C_{l_α}. The vertical tail damage mainly results in a steady change in lateral forces and directional stability indicated by the values of C_{Y_β}, C_{n_β}, and C_{n_r} [30]. For the wing damage experiments conducted in [14,15], the most important observation is the reduced lift force and the incremental rolling moment induced by unequal normal force contributions from left to right wings. Also, the effective dihedral C_{l_β} is affected due to wingtip loss.

Another important conclusion from the experimental data is that the changed aerodynamic coefficients can be simply approximated by magnitude scaling, and the change scale on different levels of damage can be calculated as follows:

$$\text{change scale } \Delta C = \frac{C_{\text{damaged}} - C_{\text{undamaged}}}{|C_{\text{undamaged}}|} \cdot 100\% \qquad (4)$$

By analyzing the wind-tunnel data, it can be assumed that the relation between the change scale of each aerodynamic coefficient and the percentage of tip loss is approximately linear. Therefore, in order to model the change scale of coefficients for different levels of damage, linear interpolation is used, based on the calculated change scales of experiment data [14–16,30]. In this paper, five damage levels ranging from 10 to 50% are modeled for each of the three typical damage locations on the Cessna Citation aircraft. The interpolated change scales of each affected stability derivative under various damage levels are listed in Table 1. In our simulation environment of the Cessna Citation aircraft (DASMAT), the aerodynamic model is stored in the form of lookup tables. The aerodynamic model for the damaged aircraft is obtained by a linear scaling of the nominal model according to the interpolated change scales listed in Table 1:

$$C_{X_{\mathrm{dmg}}} = (1 + \Delta C_X)C_{X_0} \qquad C_{Y_{\mathrm{dmg}}} = (1 + \Delta C_Y)C_{Y_0} \quad C_{Z_{\mathrm{dmg}}} = (1 + \Delta C_Z)C_{Z_0}$$
$$C_{l_{\mathrm{dmg}}} = (1 + \Delta C_l)C_{l_0} + \Delta C_{l_\alpha}\alpha \quad C_{m_{\mathrm{dmg}}} = (1 + \Delta C_m)C_{m_0} \quad C_{n_{\mathrm{dmg}}} = (1 + \Delta C_n)C_{n_0} \qquad (5)$$

where, for example, C_{X_0} denotes the original value in the lookup table of DASMAT, and $C_{X_{\mathrm{dmg}}}$ denotes the modeled value for the damaged Cessna Citation aircraft. The outputs of the nominal and damaged models are shown in Figs. 4–6, where the nominal model outputs are directly retrieved from the aerodynamic lookup table. The modeled aerodynamic effects of the Cessna Citation display similar patterns to the wind-tunnel results in [14–16] because they share similar configurations.

B. Anomaly Detection

Anomaly detection refers to the problem of finding patterns in the data that do not conform with expected behaviors. In this research, anomalies are defined as abnormal values of observed aerodynamic forces and moments that may indicate the occurrence of structural damage. The basic idea is to fit a probability distribution into the training set of normal data, based on which the data points that have very low probabilities are labeled as anomalies [31].

In this paper, the normal data and abnormal data are defined, respectively, as the measured dimensionless forces and moments of undamaged and damaged aircraft. If the residual $r(t)$ denotes the difference between the measured output $y(t)$ and an estimated output $\hat{y}(t)$ computed based on the aerodynamic model [i.e., $r(t) = y(t) - \hat{y}(t)$], the mean of the residual $E[r(t)]$ should be zero in the no-damage case; otherwise, it will deviate from zero. In reality, however, the residuals are corrupted by noise, unknown disturbances, and uncertainties in the system model [12]. Therefore, the distribution of the residual is used as the criterion for anomaly detection because the output residual during undamaged flight can be expected to have statistics determined by the noise present in the system [32].

As illustrated in Fig. 7, the distribution of the residual is calculated using data from a series of experiments on the undamaged aircraft. Each training data point is the absolute value of the residual, which is used to fit a certain distribution (e.g., Gaussian) by calculating the parameters of its probability density function (PDF). The trained PDF is then used to evaluate the probability density of newly measured data and decide whether it contains anomalies or not. Take Gaussian distribution, for example; the probability density of each incoming new data point $p(r_{\mathrm{new}})$ is computed according to the following:

$$p(r_{\mathrm{new}}|\mu, \sigma) = \frac{1}{\sqrt{2\pi\sigma^2}}\exp\left(-\frac{(r_{\mathrm{new}} - \mu)^2}{2\sigma^2}\right) \qquad (6)$$

where μ and σ are the trained parameters of the Gaussian distribution of the undamaged aircraft. When damage occurs, the sudden change of forces and moments will result in a residual that has a very low probability in the distribution of normal data. Anomalies can then be detected using a threshold, where $y = 1$ signifies the potential existence of an anomaly:

$$y = \begin{cases} 1 & \text{if } p(r_{\mathrm{new}}) < \varepsilon(\text{anomaly}) \\ 0 & \text{if } p(r_{\mathrm{new}}) > \varepsilon(\text{normal}) \end{cases} \qquad (7)$$

The threshold ε is determined based on a cross-validation set of labeled examples, including both normal and abnormal data points

[31]. Because each of the six dimensionless forces and moments has a separate channel, the anomaly detection can be processed separately for each channel based on one of the six thresholds, which will be combined to trigger the damage classification process discussed in the next section.

C. Damage Classification Using Neural Networks

If the anomaly detection algorithm indicates the existence of damage, further steps should be taken to find the location of the damage to the horizontal stabilizers, wings, and the vertical tail; and subsequently assess the damage severity. However, two problems exist. One problem is that there is no explicit mapping, i.e., a precise analytic mathematical function that describes the relationship between the damage condition of the aircraft and the changed aerodynamic characteristics of the damaged aircraft. The second problem is that, even if the damage severity could be estimated in an analytic form, it may take one of infinite values between 0 and 100%, which makes database building and retrieval of the corresponding SFE impractical. These problems are tackled in this paper by using pattern classification techniques, where "patterns" or "classes" specifically indicate the damage situation of the aircraft represented by discrete values with a chosen interval (e.g., 10, 20, 30%, ...). In this way, the entire range of damage severity is decomposed into small segments so that the damage severity can be approximated by these discrete values. Furthermore, the mapping from identified aerodynamic coefficients to the damage conditions can be learned from a training process. Therefore, the current damage condition is estimated without explicit functions. The essential part of any pattern classification method is the training of the mapping from a dataset $\mathcal{X}$ to its assigned class label set $\mathcal{Y}$:

$$f : \mathcal{X} \to \mathcal{Y} \qquad (8)$$

The class label set $\mathcal{Y}$, or target set, contains k vectors $\boldsymbol{y}$ corresponding to k potential damage cases (e.g., 20% tip loss of the left wing). The dataset $\mathcal{X}$ consists of m vectors $\boldsymbol{x}$ collected from m experiments, and each n-dimensional vector $\boldsymbol{x}^{(m)}$ contains n extracted features, which are specifically defined in this paper as the stability derivatives (e.g., C_{m_α}, C_{m_q}) identified from each of the k damage cases. If $k = 2$ and $\boldsymbol{y} \in \{0, 1\}$, the problem is reduced to binary classification. Many methods are well developed for binary classification, such as logistic regression and support vector machines [20,33], and each method has different ways of computing decision boundaries. In our research, however, more than two damage cases need to be isolated and classified, which turns the problem into multiclass classification. This kind of problem can be solved by decomposition into several binary classification tasks that can be solved efficiently using binary classifiers. In general, there are two binarization schemes that are most widely used: one vs all, and one vs one. Literature can be found comparing these schemes with various binary classifiers, and both of them have their pros and cons, depending on the classifier used and the size of the training set [34].

In this paper, a multilayer neural network is used for classification. One major difference of the neural network from other classifiers is that it can deal with multiclass classification problems by a single

Table 1   Changed value of dimensionless forces and moments due to different levels of damage

Damage severity, %	Left horizontal stabilizer tip loss			Vertical tail tip loss			Left wingtip loss		
	ΔC_{m_α}, %	ΔC_{m_q}, %	ΔC_{l_α}, %	ΔC_{n_β}, %	ΔC_{Y_β}, %	ΔC_{n_r}, %	ΔC_{L_α}, %	ΔC_{l_β}, %	ΔC_{l_α}, %
10	15	8	−3	−25	8	20	−5	10	−10
20	25	15	−5	−40	15	30	−10	10	−10
30	30	20	−10	−50	25	40	−15	30	−28
40	45	30	−12	−60	30	50	−20	40	−36
50	57	43	−15	−70	40	60	−25	50	−45

a) Static longitudinal stability   b) Pitch damping   c) Incremental rolling moment versus angle of attack
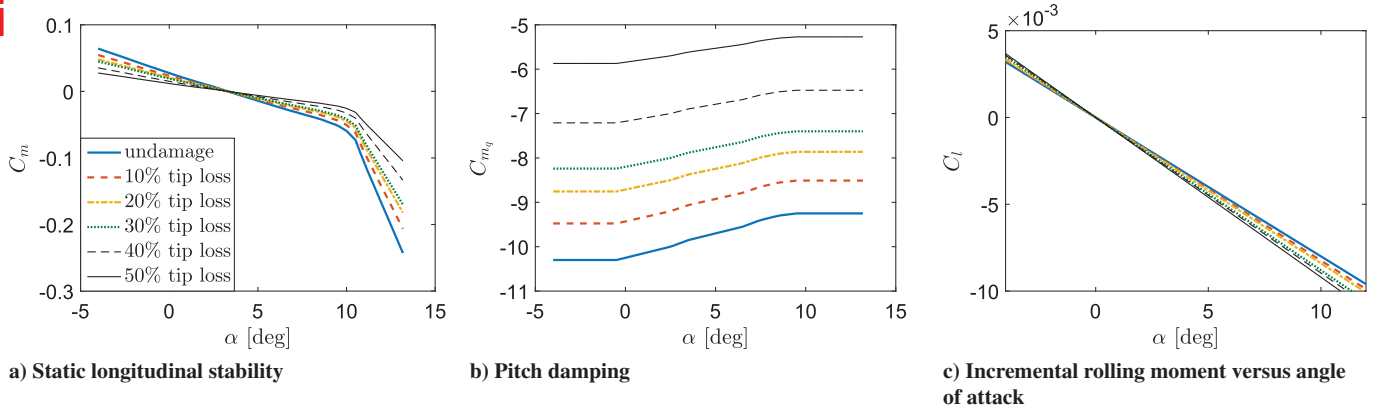
Fig. 4   Aerodynamic effects of different levels of horizontal stabilizer damage.

a) Static directional stability   b) Lateral force versus sideslip   c) Yaw damping
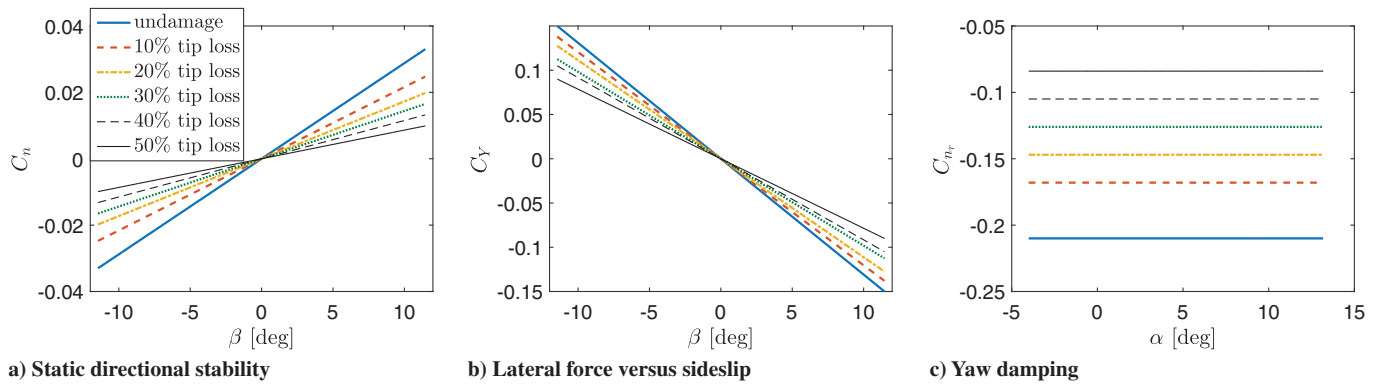
Fig. 5   Aerodynamic effects of different levels of vertical tail damage.

a) Lift coefficient   b) Dihedral effect   c) Incremental rolling moment versus angle of attack
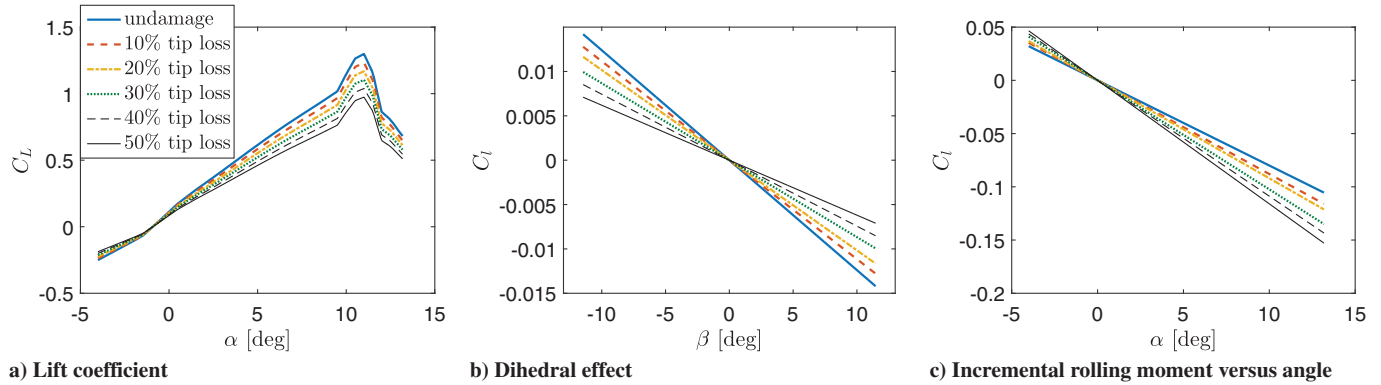
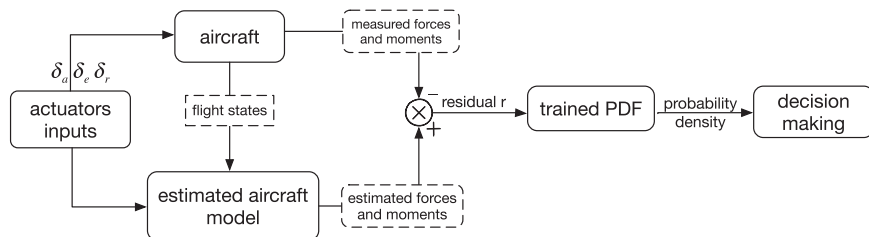Fig. 6   Aerodynamic effects of different levels of wing damage.

Fig. 7   Anomaly detection process during flight simulations.

network structure [34,35], where each input unit represents one of the features in the vector x, and each output label defined as $y \in \Re^k$ represents one of the k classes by setting only one element in the vector to be one. A multilayer neural network [20] consists of one input layer, several hidden layers, and an output layer, which are all interconnected by modifiable weights; and a single bias unit that is connected to each unit other than the input units. Nonlinear multilayer networks have great approximation power and can implement arbitrary decision boundaries. The decision regions need not be convex nor simply connected. The neural networks have two

primary modes of operation: evaluation and learning. For evaluation, the input is simply passed through the network to the output layer. For supervised learning of the network, the network parameters (i.e., weights) are modified such that the network output converges toward a target output. For training the weights of the multilayer networks, the backpropagation algorithm is used [20].

When structural damage occurs, some representative stability derivatives are extracted from the identified models as features for damage classification. The identified parameters in every simulated flight test form a training set for each typical damage case, which is used to generate decision boundaries during the training process. The richness of the training set is one of the key factors that determine the accuracy of the classification results. If the number of classes is too small, the estimation of the actual situation can be coarse and inaccurate, whereas too many classes may lead to the problem of ambiguity and complex implementations. Hence, the designed number of classes in the training set is a tradeoff between desired numerical accuracy and physical restrictions. For each new feature vector $x_{new} \in \mathcal{X}$ extracted from an unknown damage case, the classification can be performed by finding out its class label $y_{new} \in \mathcal{Y}$ based on the trained mapping:

$$y_{new} = f(x_{new}) \tag{9}$$

In this way, the current damage severity can be classified and estimated based on the identified aerodynamic parameters. In the next section, it will be shown how the whole process is implemented via well-trained neural networks in a high-fidelity simulation environment.

V. Simulation Results

To simulate the in-flight onboard identification process, output data are generated with the open-loop DASMAT simulation model given doublet maneuvers of ± 5 deg on elevators, ailerons, and rudders triggered at different times, where the data are contaminated by measurement noise [signal-to-noise ratio (SNR) = 25]. It is important to note that, when damage happens in reality, the actuator inputs required for excitation of the system for online system identification are not specified as doublets but generated automatically by the onboard fault-tolerant controller to compensate for damage-induced excursions from the reference trajectory. In that sense, the fault-tolerant controller indirectly excites the system by making efforts to stabilize it. The incorporation of a fault-tolerant controller is currently not the scope of this paper, but it will be included in future work.

As is discussed in Sec. IV.A, the modeling of the aerodynamic effects of damage in DASMAT is based on the analysis of experimental (wind-tunnel) data. In the simulation setup, the damage cases and the corresponding changes to the dimensionless aerodynamic coefficients are listed in Table 1. It is illustrated in

Table 2   Damage parts and the corresponding stability derivatives used as features

Damage part	Features for classification
Horizontal stabilizers	C_{m_α}, C_{m_q}
Vertical tail	C_{n_β}, C_{n_r}
Wings	C_{l_α}, C_{L_α}

Fig. 8 how the training data are generated and used in the simulation of damage classification. For each damage case, the stability derivatives that have the most dominant and discernible effects are picked as classification features for the damage classifier, as listed in Table 2. These features are estimated by the system identification process described in Sec. III based on the model structure defined in Eq. (3). First, doublet maneuvers along with simulated noise are used as actuator inputs to the DASMAT model to generate the simulated responses of actual flight. The measurements of the dimensionless forces and moments C_Y, C_L, C_l, C_m, and C_n are used as inputs to the aerodynamic model identification algorithm. To test the performance of the system identification routine, three damage scenarios are designed, which are a 30% tip loss of the left horizontal stabilizer, a 20% tip loss of the vertical tail, and a 40% tip loss of the left wing.

The first two subplots of Figs. 9–11 show the time histories of dimensionless forces and moments obtained by applying a doublet maneuver of ± 5 deg on the actuators of the DASMAT simulation model. The measurements and identified values of the damaged aircraft are denoted by solid lines and dashed lines, respectively, which are compared with measurements from the undamaged aircraft in solid–dashed lines. It is observed that the identification algorithm succeeds in tracking the measured value of dimensionless forces and moments of the damaged aircraft and results in satisfactory low identification errors during the entire time span, as shown in Figs. 9c, 10c, and 11c. The identification results of the stability derivatives along with their real values are displayed in the second row of Figs. 9–11 for each of the damage cases accordingly. It is noted that the real values are extracted from the lookup table from the simulation model; but, in real flight, these cannot be directly read or measured from the aircraft. The estimated values are expected to converge to the real values during the identification process.

The ratio between the converged coefficients of the damaged and undamaged aircraft indicates the change induced by structural damage. It is clearly shown that the identified stability derivatives quickly converge to the changed values, capturing the aerodynamic characteristics accurately and providing essential information for damage classification, which is immediately triggered once the anomaly detection block gives a positive alarm. The last rows of Figs. 9–11 show the anomaly detection results of three damage cases based on the residuals between the responses of damaged and
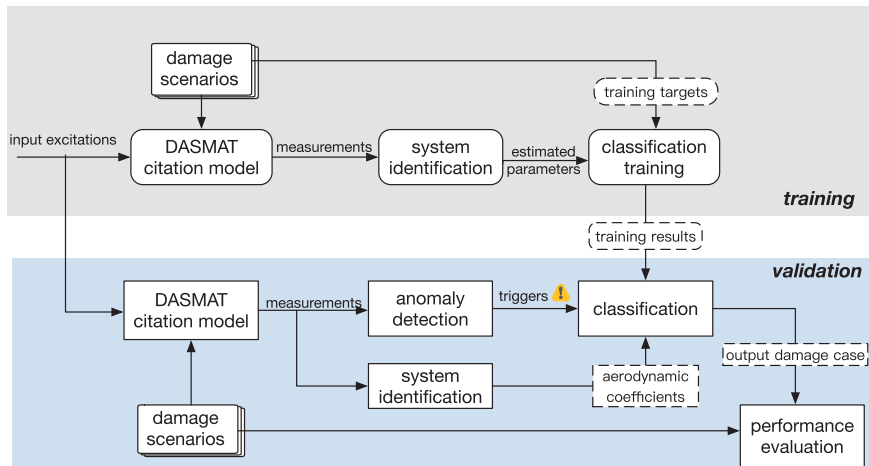

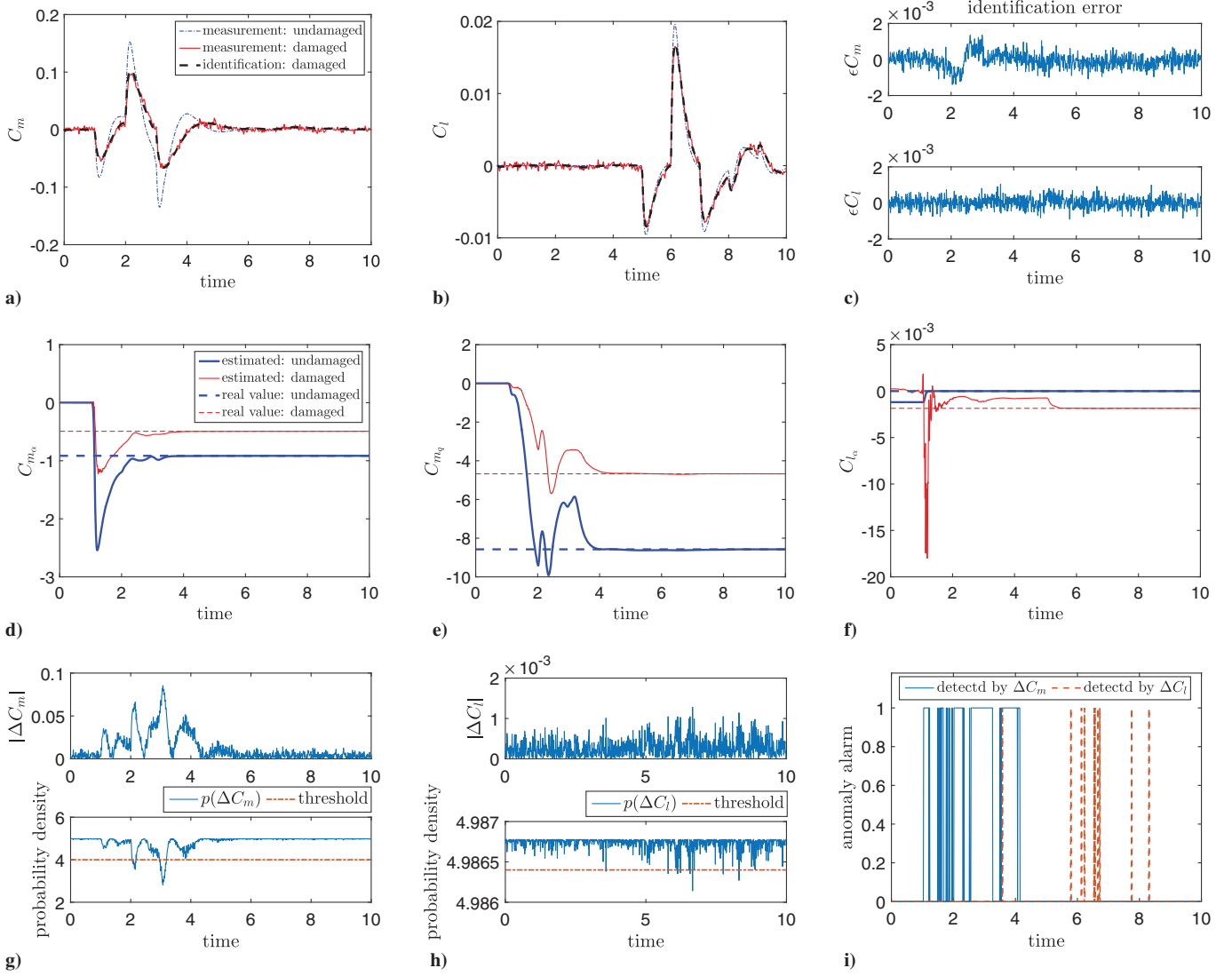**Fig. 8   Training and validation process for damage classification.**

Fig. 9   Identification and anomaly detection results of 30% tip loss of left horizontal stabilizer. The damage is triggered after 1 s.

undamaged models described in Sec. IV.B. The upper plots of Figs. 9g, 9h, 10g, 10h, 11g, and 11h depict the absolute value of residuals between measured outputs and estimated outputs with respect to time; and the probability density of the residuals computed from Eq. (5) are displayed in the lower plots. The increase of the estimation error and the corresponding decrease of its probability density is observed soon after the damage is triggered. A threshold is used to capture the anomaly observed in the data. Each channel has a separate detection threshold and different reidentification time, so the anomaly alarms are triggered individually, which are displayed in Figs. 9i, 10i, and 11i. It is important to note that, in the open-loop simulation, the time of change detection and the anomaly alarms are closely related to the time of maneuver execution of the aircraft. Hence, an updated model identified from sufficient input excitation is a key factor for a successful anomaly detection, which again leads to the future work of the application of fault-tolerant controllers in the identification loop.

The results shown in Figs. 9–11 are identification results from only one simulation experiment conducted on the DASMAT simulation model. To generate a classification dataset of 300 examples for each damage part and damage level, 5400 simulations were repeatedly run with the same input and noise level. The dataset is divided into a training set and a validation set with the proportion of 2:1, where each data vector contains two features listed in Table 2. The training builds on a base architecture of one hidden layer neural network with sigmoid functions as the activation function. The output layer has six

outputs, with the softmax function as the output transfer function. Various numbers of hidden nodes ranging from 3 to 30 were experimented with, and the performances were evaluated based on the validation data. In this simulation, the best performance is given by the neural network with 10 hidden nodes. The training results of two features based on this structure are displayed in Fig. 12, where six damage levels on three different parts of the aircraft are defined as class labels. The black markers represent the training data of different classes, and the region of each class is demonstrated. The accuracy of the training results relies on the richness of the training data. However, in real physical experiments, the generated data cannot be scattered evenly throughout the grid because data without physical meanings are unlikely to be collected in the flight simulation as training data. Hence, it is important to note that, in Fig. 12, the training result on the boundary may not be accurate due to lack of training data.

To evaluate the performance of the trained classifier, validation experiments are conducted on different damage scales for a single damage location. If data assigned to the correct class are defined as positive and the rest as negative, the validation results can be represented by four measures, which are the number of correctly classified positive data (true positive), correctly classified negative data (true negative), misclassified positive data (false positive), and misclassified negative data (false negative), respectively. Widely used criteria to evaluate classifier performance for classification problems are precision and recall, which are defined as follows [33]:
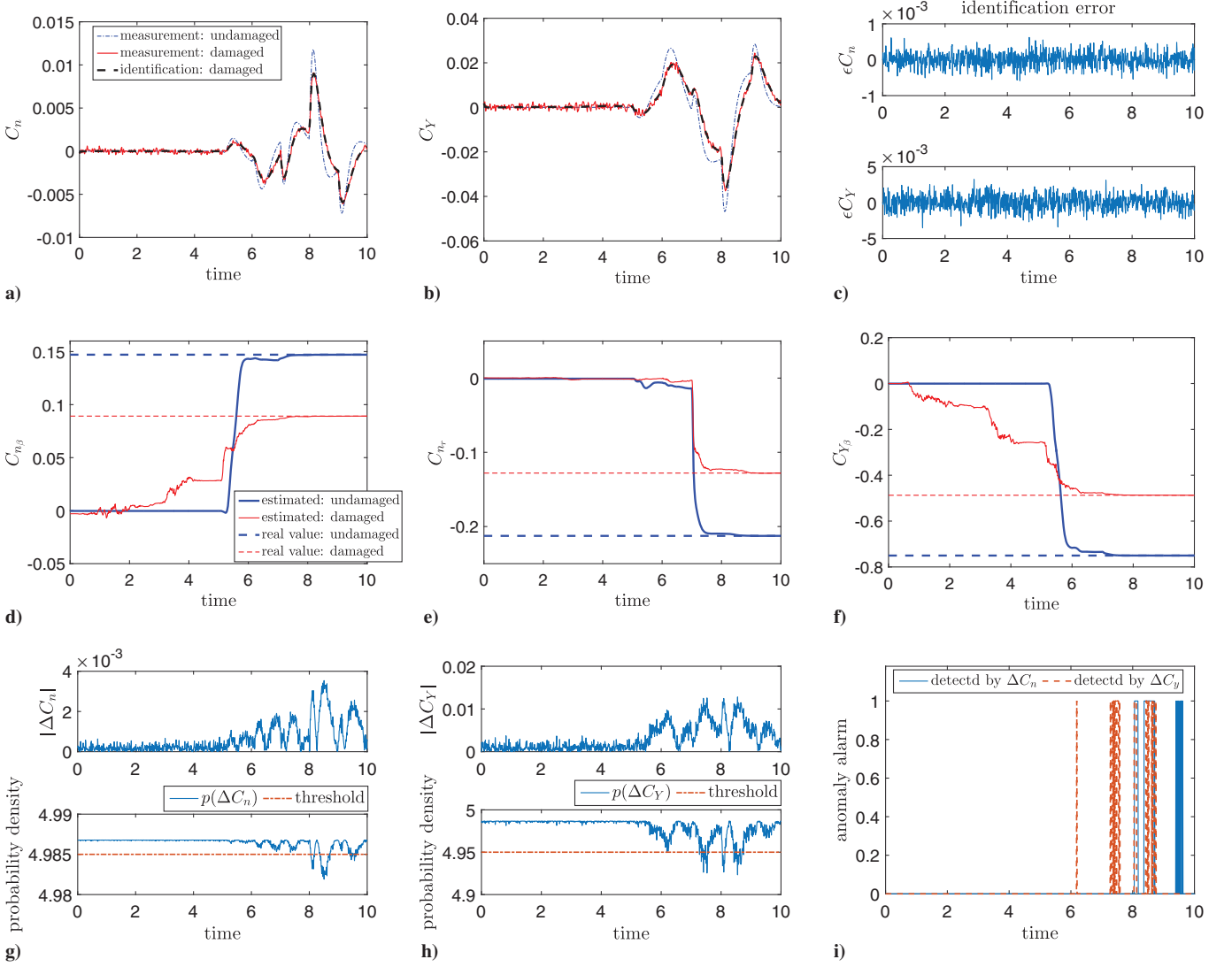
Fig. 10   Identification and anomaly detection results of 20% tip loss of vertical tail. The damage is triggered after 4 s.

$$\text{Recall} = \frac{\text{number of true positives}}{\text{number of true positives} + \text{number of false negatives}}$$

$$\text{Precision} = \frac{\text{number of true positives}}{\text{number of true positives} + \text{number of false positives}}$$

(10)

The evaluation results of the classifiers for each of the damage cases are listed in Table. 3, which shows that the damage to any of the three main parts of the Cessna Citation aircraft can be successfully detected and classified under a moderate noise level (SNR = 25).

In real flight accidents, however, structural damage may happen simultaneously to more than one location on the aircraft. Because it is impossible to list all the possible combinations that might occur, the domain of damage locations is restricted to the three major parts investigated in this paper. As was discussed in Sec. IV.A, the aerodynamic effects of damage to different parts of the aircraft are relatively independent from each other and the couplings, although they do exist, are of little impact. As a result, the combined forms of damage can be detected and classified by using separate training features, i.e., the dimensionless aerodynamic coefficients listed in Table 2. For example, if one of the horizontal stabilizers and vertical tail are damaged at the same time, the changed dimensionless moment coefficients caused by damaged horizontal stabilizers are C_m and C_l, whereas for a damaged vertical tail, the most affected dimensionless force and moment coefficients are C_Y and C_n. Hence,

alarms in these four channels will be triggered individually by the anomaly detection system. After that, the corresponding classification process will be initiated using training results displayed in Fig. 12. In this sense, the multidamage identification can be reduced to several simultaneous single-damage detection and classification problems.

VI.   Database Building and Retrieval

To support the online operations of the DEFEND system, two sets of databases are needed for damage classification and SFE prediction, respectively, which are depicted in Fig. 13. In the databases used for damage classification, each entity contains the training results based on predefined features, and the data are retrieved according to the current flight conditions. The attributes of the training results stored in the database vary in the training method and the binarization schemes that are applied offline. For a multilayer neural network, the whole network structure should be stored, including the number of layers and units, the weights between layers, and the types of activation functions, etc. Given new features with unknown labels, the training information is retrieved based on current flight conditions and new data are expected to be classified into one of the damage cases with a unique index number.

The database that contains the precalculated SFEs is a key part in the main loop of the DEFEND system, as shown in Fig. 2. The database takes in the index number of the specific damage case identified in the previous step and retrieves the corresponding SFE. Some earlier work
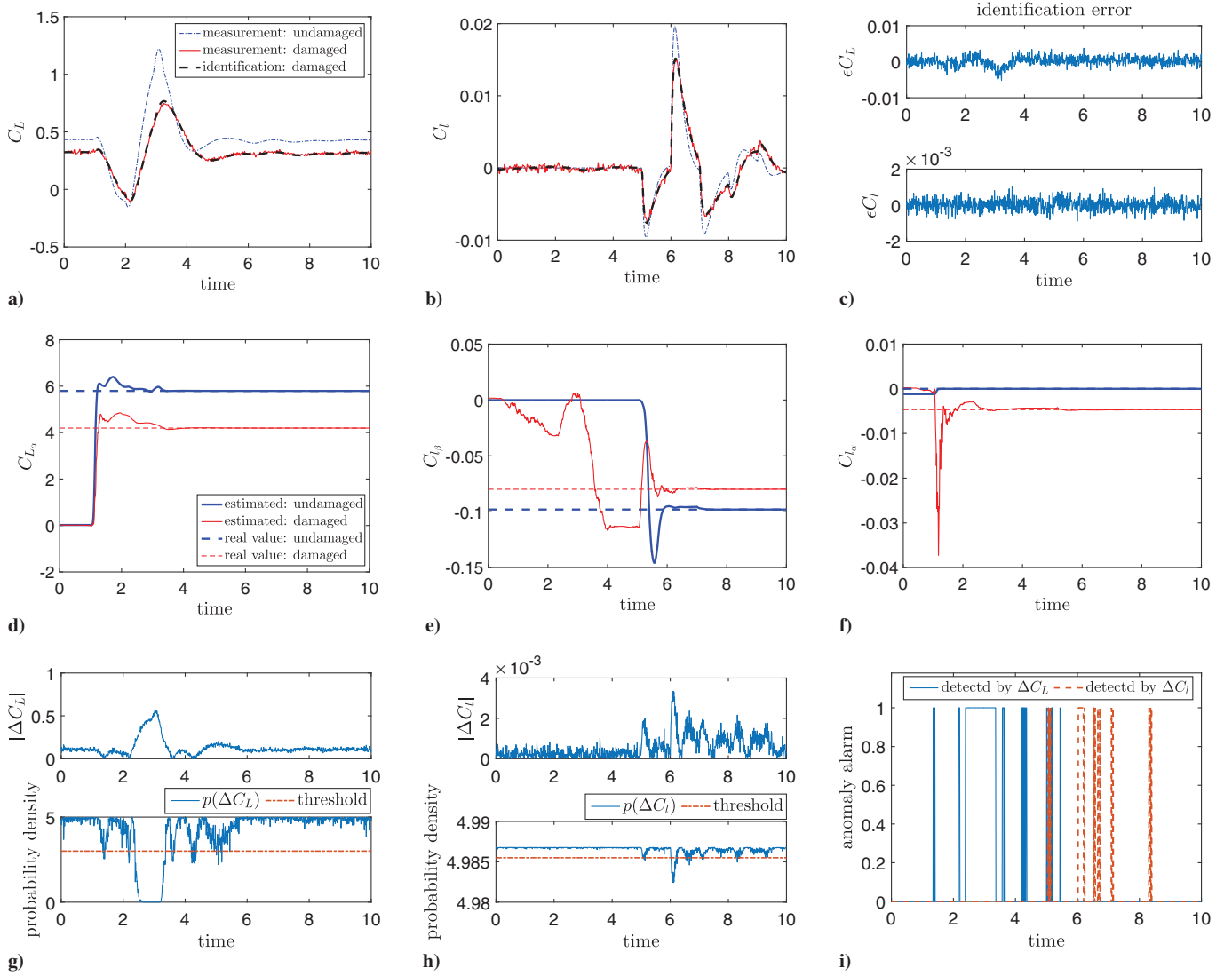
Fig. 11   Identification and anomaly detection results of 40% tip loss of left wing. The damage is triggered after 1 s.
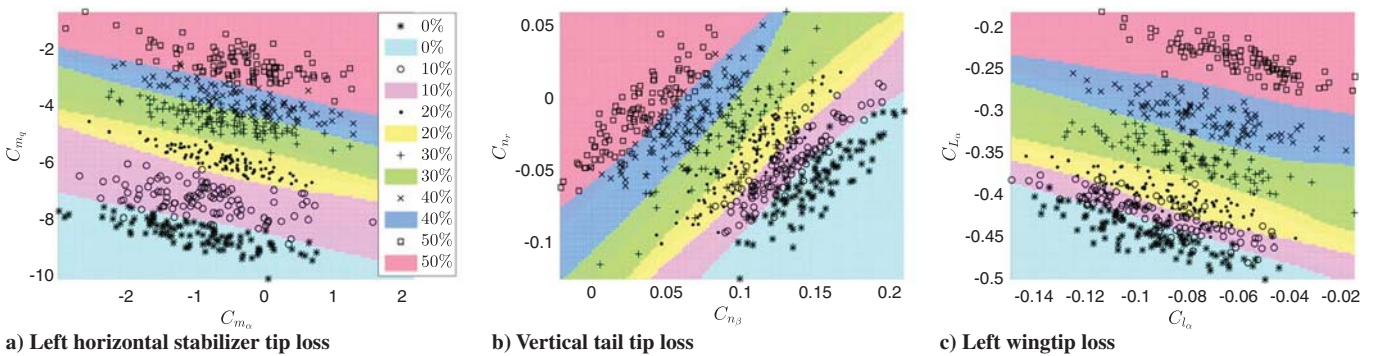

a) Left horizontal stabilizer tip loss   b) Vertical tail tip loss   c) Left wingtip loss

Fig. 12   Training results of damage severity classification in three different parts.

on the computation of SFEs can be found in [7–10,30], where SFEs are defined as the set-based intersection between the forward reachable set and the backward reachable set calculated by the level set method [5,6]. To illustrate how the changes to aerodynamic coefficients affect the shape of the SFE, an example is presented in Fig. 14 for two different scales of wing damage, from which it can be clearly seen that the changes to the aircraft model directly influence the shape of the SFE. Given certain flight conditions, one damage case in the classification training set corresponds to one SFE, which is calculated from the global models of that damage case obtained by wind-tunnel and CFD experiments. Following this method, the whole offline database of SFEs can be generated.

In real applications of database retrieval for damaged aircraft, however, safety should be included as the primary consideration in the process of transforming the classification results (i.e., the damage severity of a certain part) into the most accurate flight envelope that is guaranteed to be safe. Take wing damage, for example; suppose the actual damage is around 13% and is classified as 10% by the trained neural networks. If the classification result is directly used as the index to the database, a SFE of 10% wing damage will be retrieved, which is larger than the "true" SFE of the current 13% damage, given the fact that the SFE is continuously shrinking with increasing damage scales [30]. In this way, the retrieved SFE is less conservative and may lead to potential risks. For practical safety considerations, it

Table 3   Validation results of classification (SNR = 25)

Damage severity, %	Horizontal stabilizer		Vertical tail		Wing	
	Recall, %	Precision, %	Recall, %	Precision, %	Recall, %	Precision, %
10	95.15	98.98	96.57	98.78	98.98	97.76
20	98.94	98.51	98.65	99.88	98.61	97.89
30	99.00	99.50	97.86	98.96	99.50	95.89
40	98.02	98.50	97.58	98.66	99.50	96.98
50	99.05	99.00	99.76	98.56	99.00	99.75

may be advisable to go for the most pessimistic SFE, which points to the 20% damage level in this case. If $j_d \in \{1, 2, 3, 4, 5, 6\}$ is the index of six damage levels from the classification label set $\{0, 10, 20, 30, 40, 50\%\}$ and $j_s \in \{1, 2, 3, 4, 5, 6\}$ is the index of the corresponding SFE stored in the database, a simple but safe retrieval strategy would be like the following:

$$j_s = \begin{cases} j_d + 1 & \text{if } j_d < 6 \\ j_d & \text{if } j_d = 6 \end{cases} \qquad (11)$$

On the other hand, however, this strategy may result in overconservative and inaccurate SFEs if the interval between each class is too large. As shown in Fig. 14, the gap between the SFE of 10 and 20% damage is not trivial. It can be concluded that, the closer the discrete values of damage levels are to each other, the more accurately the SFE can be predicted. However, the number of designed damage scales is restricted by the limitations of physical experiments like wind-tunnel tests and simulations, where data are contaminated by noise. Therefore, a better approach might be through online interpolation between two or more closest SFEs retrieved from the database, as depicted in Figs. 2 and 13. The interpolation algorithm depends on the numerical method of computing the SFE and its storing format in the database, which is ongoing work. In general, the retrieval of the SFE is extremely important to the implementation of the whole DEFEND system, which will be the main focus of our future research work.

VII.   Discussion

The ultimate goal of this research is verifying the feasibility of the proposed online DEFEND system. Thus, many practical issues must be taken into consideration during the process of damage modeling and simulation design. For example, due to the formidable practical challenge of flying damaged aircraft, the model in the simulation environment is based on the wind-tunnel results of a subscale aircraft model. In the configuration of wind-tunnel experiments, the damage interval ranges from 7 to 25% tip loss for different locations [14,15], which indicates the physical limitation of making a subscale damaged aircraft and conducting wind-tunnel experiments with it. Moreover, external noise and disturbances are inevitable in real flight, which should also be modeled for the damaged aircraft. If the damage interval is too small, the aerodynamic effects will be obscured by the presence of noise and disturbances, and what is left will be a set of data that is not well suited for identification and classification. On the other hand, the number of trained damage classes and calculated SFEs largely depends on the size of designed damage intervals. By using small intervals, coarse results can be

avoided during classification and safety can be guaranteed by a more comprehensive database. Hence, in this paper, a realistic number of 10% for the interval of damage severity is chosen to verify the applicability of the proposed approach. Future research will focus on SFE interpolation in order to enhance the accuracy of the envelope predictions.

As is discussed in Sec. II, the online process of the database approach is mainly composed of three parts: system identification, damage classification, and database retrieval. The system identification and damage classification algorithms presented in this paper easily run in real time on the DASMAT flight simulator, indicating the feasibility of at least these parts of the complete system on flight hardware. The final part of the system (database retrieval) is ongoing work that will, in the near future, be verified in the real-time simulator. It should be noted that database technology by itself is a solution to fast retrieval of information from large amounts of data in real life, which are used in many applications such as search engines and online shopping [36].

This means that being efficient in real time is a dominant driving factor in the development of databases in various applications. Thus, in our DEFEND system, the current information retrieval methods are expected to provide results in real time once the database is successfully built offline. At this point in time, a database containing 108 flight envelopes has been constructed based on different damage cases and flight conditions. Preliminary work on a database setup and
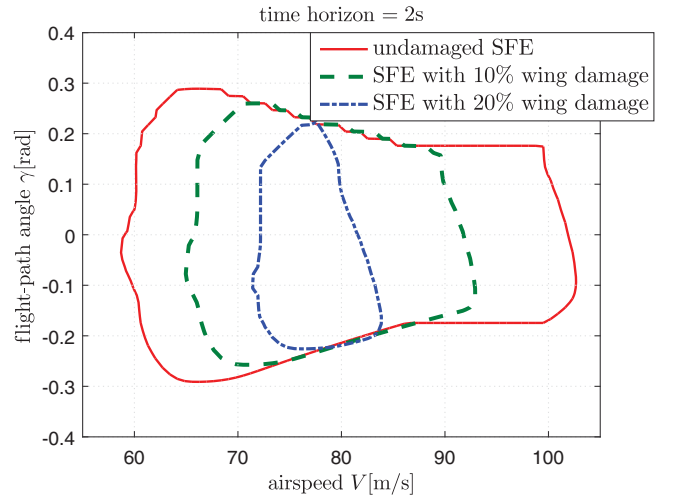
Fig. 14   Safe flight envelopes corresponding to two damage classes.
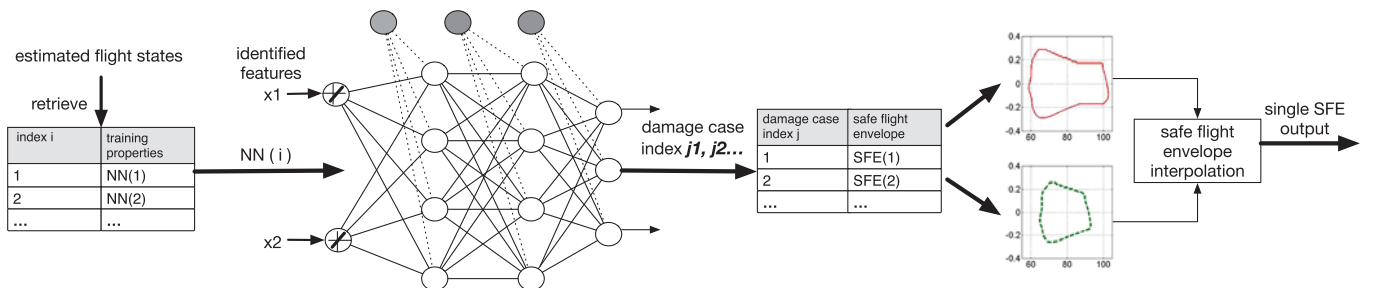
Fig. 13   Online database retrieval and safe flight-envelope interpolation.

retrieval strategy has shown the feasibility of database building offline. In the future, the database will be expanded with more data from experiments or accident investigations.

VIII.   Conclusions

A database-driven online safe flight-envelope prediction system is presented in this paper. With the aid of offline-constructed databases, challenges associated with obtaining the global model of damaged aircraft and high computational cost of safe flight-envelope prediction can be circumvented. To find the correct index to the database, pattern classification techniques are used to detect and identify the damage state of the aircraft using locally estimated stability derivatives as classification features. Finally, a general scheme for database retrieval is provided, which will close the loop for the complete envelope prediction system. It is obvious that, the more informative the database is designed to be, the higher the level of safety that can be guaranteed under damage-induced upset conditions. In this paper, three damage cases are considered as a proof of feasibility. Future work will concentrate on more real-life damage scenarios, such that the databases can be expanded to contain more damage cases. Another important issue is the interpolation of retrieved safe flight envelopes, which is a current research topic.

References

[1]   Ranter, H., "Airliner Accident Statistics 2006," Aviation Safety Network TR, 2007.

[2]   "Statistical Summary of Commercial Jet Airplane Accidents: Worldwide Operations Since 1959," The Boeing Company TR, 2009.

[3]   Russell, P., and Pardee, J., "Joint Safety Analysis Team-CAST Approved Final Report Loss of Control JSAT Results and Analysis," Federal Aviation Administration: Commercial Airline Safety Team TR, 2000.

[4]   Chongvisal, J., and Talleur, D., "Loss-of-Control Prediction and Prevention for NASA's Transport Class Model," *AIAA Guidance, Navigation, and Control Conference*, AIAA Paper 2014-0784, 2014.

[5]   Lygeros, J., "On Reachability and Minimum Cost Optimal Control," *Automatica*, Vol. 40, No. 6, 2004, pp. 917–927.
doi:10.1016/j.automatica.2004.01.012

[6]   Mitchell, I. M., "A Toolbox of Level Set Methods," Ver. 1.1, 2007.

[7]   Lombaerts, T., Schuet, S., and Wheeler, K., "Safe Maneuvering Envelope Estimation Based on a Physical Approach," *AIAA Guidance, Naviation, and Control Conference*, AIAA Paper 2013-4618, 2013.

[8]   Van Oort, E. R., "Adaptive Backstepping Control and Safety Analysis for Modern Fighter Aircraft," Ph.D. Thesis, Delft Univ. of Technology, Delft, The Netherlands, 2011.

[9]   Zhang, Y., de Visser, C. C., and Chu, Q. P., "Online Safe Flight Envelope Prediction for Damaged Aircraft: A Database-Driven Approach," *AIAA Modeling and Simulation Technologies Conference*, AIAA Paper 2016-1189, 2016.

[10]   Lombaerts, T., Schuet, S., Acosta, D., and Kaneshige, J., "On-Line Safe Flight Envelope Determination for Impaired Aircraft," *Advances in Aerospace Guidance, Navigation and Control*, edited by J. Bordeneuve-Guibé, A. Drouin, and C. Roos, 1st ed., Springer International Publishing, New York, 2015, pp. 263–282.

[11]   Lopez, I., and Sarigul-Klijn, N., "A Review of Uncertainty in Flight Vehicle Structural Damage Monitoring, Diagnosis and Control: Challenges and Opportunities," *Progress in Aerospace Sciences*, Vol. 46, No. 7, 2010, pp. 247–273.
doi:10.1016/j.paerosci.2010.03.003

[12]   Hwang, I., Kim, S., Kim, Y., and Seah, C. E., "A Survey of Fault Detection, Isolation, and Reconfiguration Methods," *IEEE Transactions on Control Systems Technology*, Vol. 18, No. 3, 2010, pp. 636–653.
doi:10.1109/TCST.2009.2026285

[13]   Lu, P., "Fault Diagnosis and Fault-Tolerant Control for Aircraft Subjected to Sensor and Actuator Faults," Ph.D. Thesis, Delft Univ. of Technology, Delft, The Netherlands, 2016.

[14]   Shah, G., "Aerodynamic Effects and Modeling of Damage to Transport Aircraft," *AIAA Atmospheric Flight Mechanics Conference and Exhibit*, AIAA Paper 2008-6203, 2008.

[15]   Shah, G., and Hill, M., "Flight Dynamics Modeling and Simulation of a Damaged Transport Aircraft," *AIAA Modeling and Simulation Technologies Conference*, AIAA Paper 2012-4632, 2012.

[16]   Shah, G., Foster, J., and Cunningham, K., "Simulation Modeling for Off-Norminal Conditions-Where are We Now?" *AIAA Modeling and Simulation Technologies Conference*, AIAA Paper 2010-7792, 2010.

[17]   Hayes, C., "Effects of Simulated Wing Damage on the Aerodynamic Characteristics of a Swept-Wing Airplane Model," NASA TM X-1550, 1968.

[18]   Tang, L., Roemer, M., Bharadwaj, S., and Belcastro, C., "An Integrated Health Assessment and Fault Contingency Management System for Aircraft," *AIAA Guidance Navigation and Control Conference*, AIAA Paper 2008-6505, 2008.

[19]   Achenbach, J. D., "Structural Health Monitoring–What is the Prescription?" *Mechanics Research Communications*, Vol. 36, No. 2, 2009, pp. 137–142.
doi:10.1016/j.mechrescom.2008.08.011

[20]   Duda, R. O., Hart, P. E., and Analysis, S., *Pattern Classification*, 2nd ed., Wiley, New York, 2000.

[21]   Mulder, J. A., Sridhar, J. K., and Breeman, J. H., *Identification of Dynamic Systems-Applications to Aircraft Part 2: Nonlinear Analysis and Manoeuvre Design*, Vol. 3, NATO, Advisory Group for Aerospace Research and Development, 1995.

[22]   Lombaerts, T., "Fault Tolerant Flight Control: A Physical Model Approach," Ph.D. Thesis, Delft Univ. of Technology, Delft, The Netherlands, 2010.

[23]   de Visser, C. C., Mulder, J., and Chu, Q. P., "A Multidimensional Spline-Based Global Nonlinear Aerodynamic Model for the Cessna Citation II," *AIAA Atmospheric Flight Mechanics Conference*, AIAA Paper 2010-7950, 2010.

[24]   Baarspul, M., Mulder, J. A., Nieuwpoort, A. H. N., and Breeman, J. H., "Mathematical Model Indentification for Flight Simulation, Based on Flight and Taxi Tests," Delft Univ. of Technology, TR LR-550, Delft, The Netherlands, 1988.

[25]   Van Der Linden, C. A. A. M., *DASMAT-Delft University Aircraft Simulation Model and Analysis Tool: A Matlab/Simulink Environment for Flight Dynamics and Control Analysis*, Series 03: Control and Simulation 03, Delft Univ. of Technology, Delft, The Netherlands, 1996.

[26]   Zhang, Y., de Visser, C. C., and Chu, Q. P., "Online Physical Model Identification for Database-Driven Safe Fight Envelope Prediction of Damaged Aircraft," *AIAA Atmospheric Flight Mechanics Conference*, AIAA Paper 2016-2011, 2016.

[27]   Tol, H. J., Visser, C. C. D., Sun, L. G., Kampen, E. V., and Chu, Q. P., "Multivariate Spline-Based Adaptive Control of High-Performance Aircraft with Aerodynamic Uncertainties," *Journal of Guidance, Control, and Dynamics*, Vol. 39, No. 4, 2016, pp. 781–800.
doi:10.2514/1.G001079

[28]   Niu, G., Son, J. D., Widodo, A., Yang, B. S., Hwang, D. H., and Kang, D.-S., "A Comparison of Classifier Performance for Fault Diagnosis of Induction Motor Using Multi-Type Signals," *Structural Health Monitoring*, Vol. 6, No. 3, 2007, pp. 215–229.
doi:10.1177/1475921707081110

[29]   Frink, N., Pirzadeh, S., and Atkins, H., "CFD Assessment of Aerodynamic Degradation of a Subsonic Transport Due to Airframe Damage," *48th AIAA Aerospace Sciences Meeting*, AIAA Paper 2010-0500, 2010.

[30]   Nabi, H. N., "Effects of Structural Failures on the Safe Flight Envelope of Aircraft," M.S. Thesis, Delft Univ. of Technology, Delft, The Netherlands, 2016.

[31]   Ng, A., "Machine Learning Lecture Notes," Stanford Univ. TR, Stanford, CA, 2014.

[32]   Lombaerts, T., Huisman, H., Chu, Q. P., Mulder, J., and Joosten, D., "Nonlinear Reconfiguring Flight Control Based on Online Physical Model Identification," *Journal of Guidance, Control, and Dynamics*, Vol. 32, No. 3, 2009, pp. 727–748.
doi:10.2514/1.40788

[33]   Abe, S., *Support Vector Machines for Pattern Classification*, Springer, New York, 2010.

[34]   Hsu, C.-W., and Lin, C.-J., "A Comparison of Methods for Multiclass Support Vector Machines," *IEEE Transactions on Neural Networks*, Vol. 13, No. 2, 2002, pp. 415–425.
doi:10.1109/72.991427

[35]   Ou, G., and Murphey, Y. L., "Multi-Class Pattern Classification Using Neural Networks," *Pattern Recognition*, Vol. 40, No. 1, 2007, pp. 4–18.
doi:10.1016/j.patcog.2006.04.041

[36]   Elmasri, R., and Navathe, S. B., *Fundamentals of Database Systems*, 6th ed., Addison-Wesley, Reading, MA, 2010.